Anisotropy of charge and spin motion in perylene hexafluoroarsenate salts

2005 J. Phys.: Condens. Matter 17 4825

(http://iopscience.iop.org/0953-8984/17/30/008)

INSTITUTE OF PHYSICS PUBLISHING JOURNAL OF PHYSICS: CONDENSED MATTER

J. Phys.: Condens. Matter **17** (2005) 4825–4832 doi:10.1088/0953-8984/17/30/008

Anisotropy of charge and spin motion in perylene hexafluoroarsenate salts

A Warth, D Saez de Jauregui and E Dormann

Physikalisches Institut, Universität Karlsruhe (TH), D-76128 Karlsruhe, Germany

Received 1 June 2005
Published 15 July 2005
Online at stacks.iop.org/JPhysCM/17/4825

Abstract

Conduction electron spin echo attenuation in well defined magnetic field gradients provides more accurate values of the anisotropy of electron spin motion than microwave conductivity measurements. The electron spin diffusion coefficient for motion along the perylene (PE) radical cation stack, $D_{\parallel}(T)$, in the PE hexafluoroarsenate salt is influenced temperature dependently by perpendicular-to-stack motion and reflects the varying average unrestricted chain length, $\bar{l}_{\parallel}(T)$. The anisotropy of $D_{\parallel}(T)$:$D_{\perp}(T)$ is larger than 7300:1 at 250 K.

1. Introduction

Radical cation salts of simple planar aromatic hydrocarbons (arenes) like naphthalene, fluoranthene, pyrene or perylene and inorganic singly charged hexafluoride anions like PF_6^- are highly anisotropic electrical conductors with a Peierls metal–nonmetal transition in the 70–230 K range and charge density wave phenomena in the low temperature range [1]. The conduction electrons which are formed from π molecular orbitals are anisotropically mobile in the metallic high temperature phase. It is a speciality of the arene radical cation salts that this mobility can be monitored experimentally by detecting the motion of the electrical charge as well as that of the electron spin. The preferred direction of motion in these quasi-one-dimensional conductors is the stacking direction of the arene radical cations.

Motion of charge and spin along one arbitrary predetermined direction is a complicated process in real quasi-one-dimensional conductors. Even for motion along the preferred direction, obstacles encountered along the path define a restricted, finite chain length $l_{\parallel}$ and have to be by-passed by means of the unfavourable perpendicular-to-stack motion, probably of hopping type [2]. Thus, in fluoranthene organic conductors, the conduction electron spin (self-) diffusion coefficient $D_{\parallel}$ seemed to reflect a structural phase transition at T_s, about 200–210 K, which is 20 K above the Peierls transition that modifies only the arrangement of the molecular units perpendicular to the stacking direction [3]. The supposition that the perpendicular-to-stack motion (and its modification by structural phase transitions) is generally also relevant for the measured, presumed parallel-to stack motion for quasi-one-dimensional conductors, built up with radical cations of planar aromatic pure hydrocarbon molecules (arenes), will be

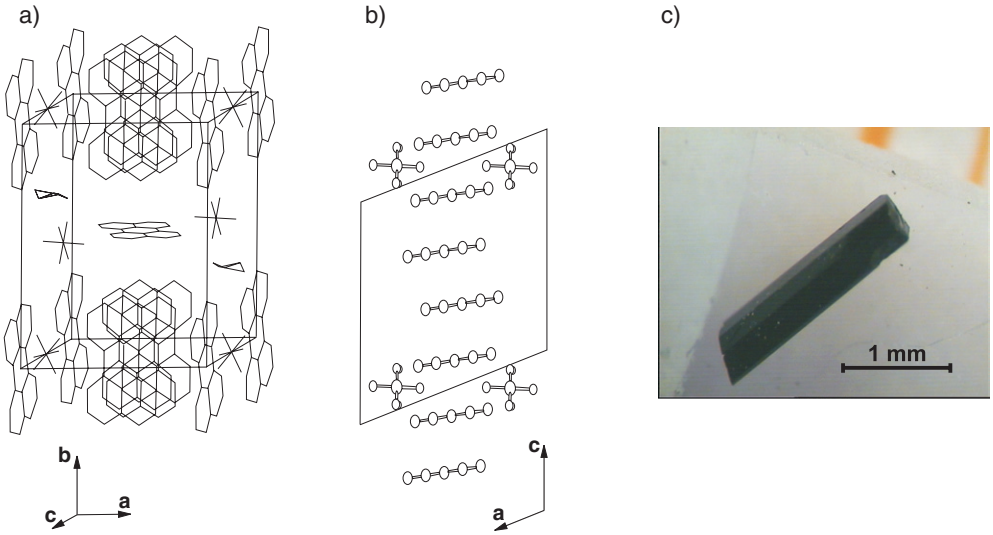

Figure 1. Crystal structure of $(PE)_2AsF_6 \cdot \frac{2}{3}THF$ seen along the stacking direction (a) and perpendicular to the stacking direction (b), as well as optically (c).
(This figure is in colour only in the electronic version)

examined here for a perylene radical cation salt, of which the crystal structure is shown in figure 1 [4].

The experimental characterization of the anisotropy of charge and spin motion is not at all trivial. In order to specify the temperature and orientation dependence of the electrical conductivity only a measurement with a contactless method like the microwave conductivity measurement with the cavity perturbation method can be used [5]. Even in this technique, the limit of the distinction between the parallel-to-stack or perpendicular-to-stack charge motion is set instrumentally, because the non-ellipsoidal shape of the single crystals (figure 1(c)) results in non-uniform depolarization fields. This typically limits anisotropy studies to a 100:1 ratio of $\sigma_\parallel$:$\sigma_\perp$, as exemplified in figure 2, and introduces mixtures of both temperature dependences into the presumably separated $\sigma_\parallel(T)$ and $\sigma_\perp(T)$ data sets. Yet just the precise temperature dependence of $\sigma_\perp(T)$ would allow us to distinguish between different models of the perpendicular-to-stack motion and of conduction electron description in quasi-one-dimensional conductors. Fortunately, the carrier motion in arene radical cation salts can also be detected via their spin diffusion coefficient $D(\theta)$. Some clarifying remarks on the terminology are required here. 'Spin diffusion' is also a well known phenomenon in quasi-one-dimensional magnetic systems with localized unpaired spins. By a 'flip–flop' process, the Zeeman energy can migrate through the sample. For quasi-one-dimensional exchange coupled systems, this type of spin diffusion is recognized on the basis of the non-exponential free induction or spin-echo decay even in homogeneous magnetic fields and, analogously, with the help of the electron spin resonance line shape's deviation from the Lorentzian form in a continuous wave experiment. No such anomalies were observed for arene salts [6], and estimates show that the dipolar contribution to D is less efficient by many orders of magnitude than the spin diffusion via carrier motion [7]. The latter corresponds to the so-called 'self-diffusion', well known from nuclear magnetic resonance in liquids [8]. The diffusive motion of the entity that carries the spin can easily be quantified from the spin-echo decay in a magnetic field gradient G of well defined direction and strength, because it gives rise to an additional damping of the spin

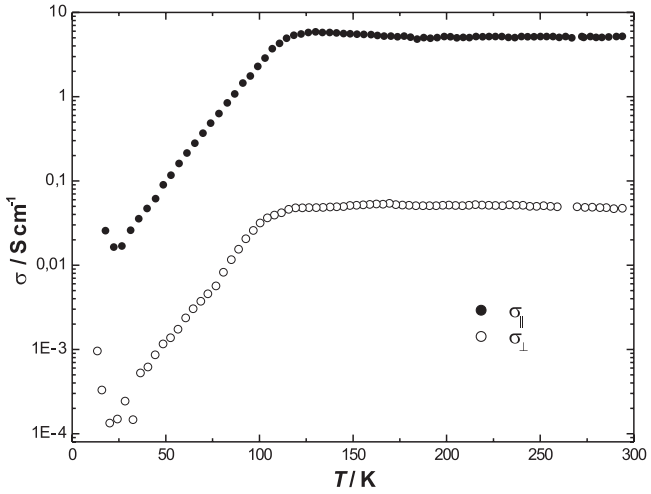

Figure 2. Microwave conductivity (10 GHz) of $(PE)_2AsF_6 \cdot \frac{2}{3}THF$ (sample A) versus temperature.

echo beyond the decay caused by relaxation processes by a factor depending exponentially on $\frac{2}{3}\gamma^2 D G^2 \tau^3$ (with gyromagnetic ratio γ and pulse separation τ) [8]. For free diffusion in the quasi-one-dimensional conductors, $(D_\parallel G_\parallel^2 + D_\perp G_\perp^2)\tau^3$ in the damping factor gives access to the anisotropy of the diffusive motion [9]. The study of the anisotropy of the spin motion (or diffusion coefficient $D(\theta, T)$) is less subject to instrumental limitation, because demagnetization fields are negligible in radical cation salts of simple arenes [4]. Thus the proof of an anisotropy of at least 2000:1 for $D_\parallel : D_\perp$ for fluoranthene salts could be realized by analysis of the anisotropy of the electron spin-echo decay in a static magnetic field gradient [10].

The perylene (PE) hexafluoroarsenate salt was selected for the present investigation [4, 6, 11–16]. It has an unusually wide temperature separation between the (second order) structural phase transition at $T_s \approx 171$ K, where the arrangement of the perylene molecules perpendicular to the stacks is modified [12], and the subsequent Peierls transition at $T_P \approx 102$ K, where the conductivity decrease is more pronounced (figure 2) and a static energy gap is opened at the Fermi level [4, 13]. The main disadvantage of this sample choice is the somewhat complicated crystal structure (figure 1) with neutral PE molecules surrounding the conducting stacks, i.e. $(PE)_4^{3+\bullet\bullet\bullet}(PE)_2^0(AsF_6^-)_3 \cdot 2$ [tetrahydrofuran (THF)] [14, 15], and with solvent inclusion in the unit cell. Due to the disordered solvent molecule site occupation the carrier motion in this radical cation salt must be modelled with a probability distribution of restricted chain lengths $l_\parallel$ [11, 16]:

$$p(l_\parallel) = \bar{l}_\parallel^{-1} \exp(-l_\parallel / \bar{l}_\parallel) \tag{1}$$

with an average value of the exponential chain length distribution $\bar{l}_\parallel$ of 80–150 μm. Fortunately, the length $\bar{l}_\parallel$ can be derived from the quantitative description of the short as well as the long time behaviour of the spin-echo decay in the magnetic field gradient G, thus the temperature dependence of $\bar{l}_\parallel(T)$ is also accessible. The same crystal is used for microwave conductivity and spin diffusion coefficient measurement in the current analysis.

In this report we mention briefly the experimental details and data analysis in section 2, discuss the normalized temperature dependences of $\sigma_\parallel$, $\sigma_\perp$, $D_\parallel$, $D_\perp$ and $\bar{l}_\parallel$ in section 3 and present our conclusions in section 4.

Table 1. Parameters of $(PE)_2AsF_6 \cdot \frac{2}{3}THF$ samples (for details see the text). (Sample dimensions A: 0.34 × 0.61 × 2.32(0.85) mm^3 (in brackets: shortened for measurement of $D(\theta)$). Sample dimensions B: 0.44 × 0.56 × 0.32 mm^3.)

	Sample A	Sample B
$\sigma_\parallel$ (250 K)	5.2 S cm^{-1}	—
$\sigma_\perp$ (250 K)	0.05 S cm^{-1}	—
$D_\parallel$ (250 K)	0.6 cm^2 s^{-1}	0.7 cm^2 s^{-1}
$\bar{l}_\parallel$ (250 K)	117 μm	81 μm
T_2 (0°, 250 K)	1.6 μs	2.2 μs
T_2 (90°, 250 K)	3.2 μs	3.7 μs
x_d	1.2%/fu	—
$D_\perp$ (250 K)	$<1.4 \times 10^{-4}$ cm^2 s^{-1}	$\leqslant 9.9 \times 10^{-5}$ cm^2 s^{-1}

2. Experimental details

Single crystals of $(PE)_2AsF_6 \cdot \frac{2}{3}$ THF were grown by electrocrystallization from THF solution as described earlier [4]. Figure 1(c) shows one example. We mainly discuss results derived for one selected crystal, sample 'A', characterized in table 1. Microwave conductivity was determined at 10.15 GHz for $\sigma_\parallel$ and 10.3 GHz for $\sigma_\perp$ using the cavity perturbation method [5, 13]. Figure 2 shows the results for sample A on a logarithmic scale. The linear scale used for representing the normalized data in figure 4 exhibits the relative decrease of $\sigma_\perp(T)$ for $T_P < T < T_s$ more clearly. Using the most pronounced anomaly of $d(\ln\sigma)/d(1/T)$ as criterion, $T_P = 103$ K is derived for sample A. The experimental limit of the anisotropy $\sigma_\parallel/\sigma_\perp$ amounts only to 100:1 for this sample.

The spin diffusion coefficient $D_\parallel(T)$ and $D_\perp(T)$ defined by

$$\langle r_i^2 \rangle = 2D_i \cdot t \tag{2}$$

(with $i = \parallel, \perp$) was derived from a joint quantitative analysis of the various spin-echo decays $A(2\tau)$ for varied θ values at the same temperature in a fixed static magnetic field gradient G, with $G_\parallel = G\cos\theta$ and $G_\perp = G\sin\theta$, $\theta = 0$ for the stacking axis, and orientation dependent transversal relaxation time $T_2(\theta)$, see [10] for details of the lengthy mathematical expression:

$$\frac{A(l_\parallel, l_\perp, 2\tau)}{A(l_\parallel, l_\perp, 0)} = \exp(-2\tau/T_2(\theta))F(G_\parallel^2, D_\parallel, l_\parallel, \tau) \times F(G_\perp^2, D_\perp, l_\perp, \tau). \tag{3}$$

Whereas $D_\perp$ is so small that the assumption of $l_\perp = \infty$ gives no reduction of the fit quality, for the $\parallel$ direction folding with the length distribution of $l_\parallel$ (equation (1)) is necessary and time consuming.

The arrangement of two iron wedges creating the field gradient installed on the two opposite sides of both pole caps of the electromagnet was characterized quantitatively. This arrangement gave a gradient $G = 1.001 \pm 0.011$ T m^{-1} perpendicular to the main field direction and allowed us to push the limit of $D_\parallel{:}D_\perp$ to 5500:1 for crystals of up to 1 mm length [17]. Figure 3 shows that the improved gradient control and the very careful data modelling optimization allows a quantitative description of the conduction electron spin-echo decay and its orientation dependence with one set of parameters (table 1). The normalized temperature dependence of the parameters relevant for the subsequent discussion is shown in figure 4 for sample A.

Arene radical cation salt single crystals exhibit a distribution of T_2 values for fixed orientation due to the variation of the local impurity concentration during electro-chemical crystal growth [18]. Thus the actual error for the anisotropy of $D_\parallel{:}D_\perp$ was increased, and the

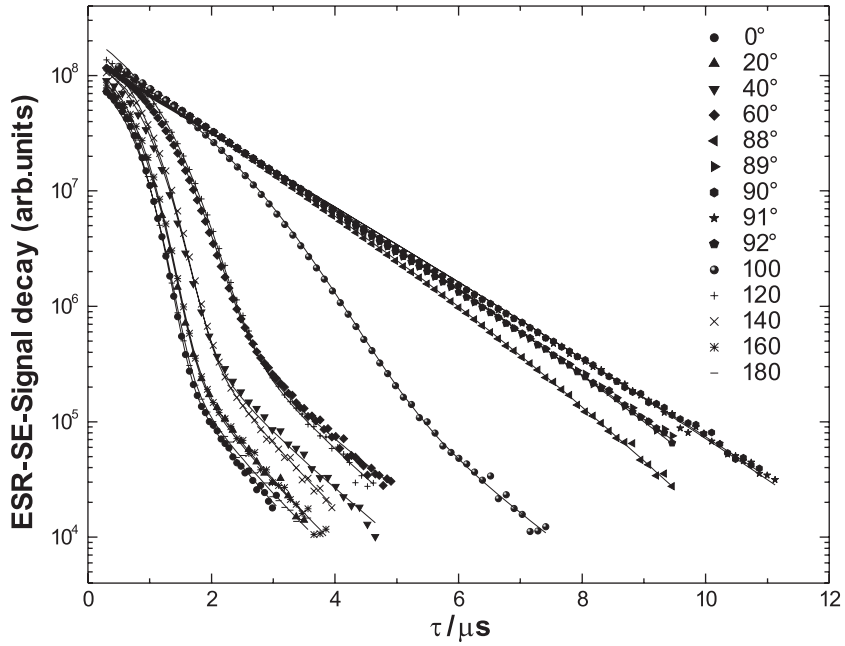

Figure 3. Orientation dependence of conduction electron spin-echo decay for $(PE)_2AsF_6 \cdot \frac{2}{3}THF$ at 9.5 GHz and in a field gradient of 1 T m^{-1} ($T = 250$ K). The solid line fit is explained in text.

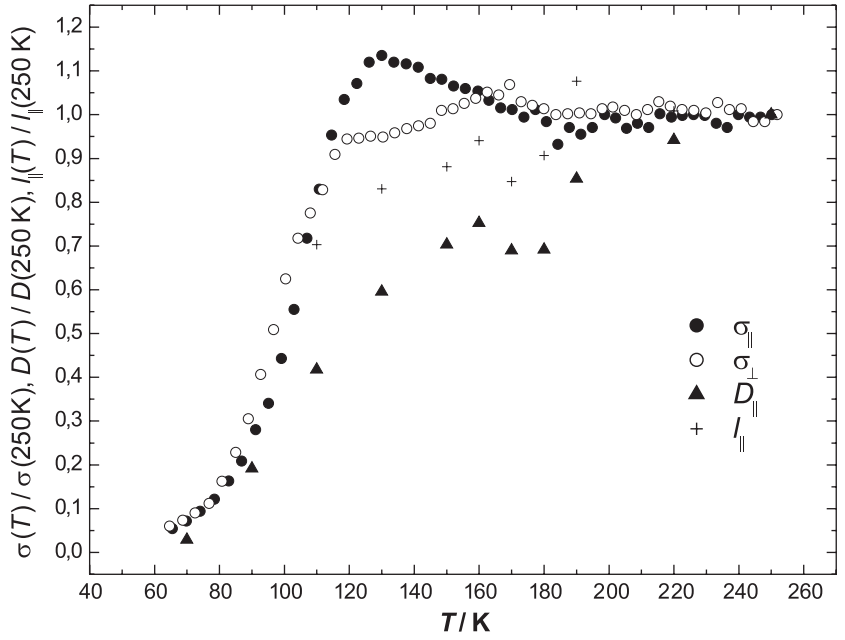

Figure 4. Normalized temperature dependence of microwave conductivity $\sigma_\parallel$ and $\sigma_\perp$, electron spin self-diffusion coefficient $D_\parallel$ and average unrestricted chain length $\overline{l}_\parallel$ for sample A of $(PE)_2AsF_6 \cdot \frac{2}{3}THF$. For absolute values see table 1.

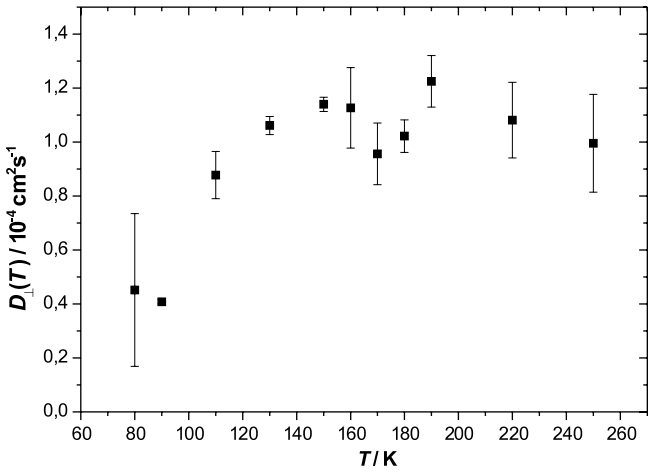

Figure 5. Temperature dependence of conduction electron diffusion coefficient perpendicular to stacking direction, $D_\perp(T)$, of $(PE)_2AsF_6{\cdot}\frac{2}{3}THF$, sample B.

limit of only 4200:1 for sample A is due to the deviation from monoexponential T_2 decay of the echo amplitude even for $\theta = 90°$. In order to derive the limiting $D_\perp(T)$ behaviour, thin slices of $(PE)_2AsF_6{\cdot}\frac{2}{3}$ THF single crystals were prepared in analogy to [7] in order to reduce the influence of transverse components of the field gradient [10]. The $D_\perp(T)$ data included in figure 5 and table 1 for sample B were derived by separating the influence of spatially varying (i) T_2^i on the spin-echo decay by means of a variation of the strength of the static field gradient $G_\perp$ in

$$A(2\tau) = \left(\sum_i A^i(0)\exp\left\{-\frac{2\tau}{T_2^i}\right\}\right)\cdot\exp\left\{-\frac{2}{3}D_\perp\gamma^2G_\perp^2\tau^3\right\} \tag{4}$$

up to $G = 2.8\ \mathrm{T\ m^{-1}}$ as was done in earlier experiments [11]. Evidently the value of $D_\perp$ (250 K) obtained from the long-time limit in equation (4) for sample B is lower than the limit obtained for sample A.

A parameter that is useful for a comparison of different sample qualities is the total concentration of $S = 1/2$ localized Curie paramagnetic defects, x_d, measured at low temperature with absolute intensity calibration in continuous wave electron spin resonance. This parameter, derived at the end of all other measurements, is included in table 1 for sample A.

3. Discussion

The large temperature separation between the Peierls transition at $T_P = 103$ K and the structural phase transition at $T_s = 171$ K for the $(PE)_2AsF_6{\cdot}\frac{2}{3}THF$ salt can now be exploited for a better understanding of carrier motion in quasi-one-dimensional conductors. We focus on figure 4 for ease of comparison.

For temperatures above T_s, microwave conductivity $(\sigma_\parallel, \sigma_\perp)$, diffusion coefficient $D_\parallel$, and average restricted chain length, $\overline{l}_\parallel$, are essentially independent of temperature. Clear differences are seen in the temperature range $T_P < T < T_s$. Whereas $\sigma_\parallel(T)$ increases metallically with decreasing T down to $T \approx 130$ K, $\sigma_\perp(T)$ decreases, as does $D_\parallel(T)$ but even more pronounced. Below T_P, the similarity of the T dependences of $\sigma_\parallel$, $\sigma_\perp$ and $D_\parallel$ is recovered.

A most important result of the quantitative data analysis is the parameter $\overline{l}_{\parallel}(T)$, because the restriction of diffusion of the electron spins along the stacking direction in $(PE)_2AsF_6{\cdot}\frac{2}{3}$ THF is reflected by the average chain length $\overline{l}_{\parallel}$ plotted in figure 4. $\overline{l}_{\parallel}(T)$ evidently decreases substantially below the structural phase transition, $T < T_s$, where domains with varying PE stack rotation are formed. The conduction electron spin diffusion coefficient $D_{\parallel}(T)$ is reasonably large in $(PE)_2AsF_6{\cdot}\frac{2}{3}$ THF crystals of typical quality, reaching $D_{\parallel}(250\ \mathrm{K}) \approx 0.6\ \mathrm{cm}^2\ \mathrm{s}^{-1}$. Thus restrictions to one-dimensional free diffusive motion with an average of $\overline{l}_{\parallel} = 100\ \mu\mathrm{m}$ for their exponential chain length distribution are sensed in static gradient spin echo attenuation experiments spanning time intervals up to $2\tau = 8$–$10\ \mu\mathrm{s}$ (or $\tau = 4$–$5\ \mu\mathrm{s}$, on the scale shown in figure 3). Indeed, a root mean square path length of 35 μm is calculated with equation (2). For the microwave conductivity at 10 GHz, 'free' space for the (charge) motion of the conduction electrons is required for 50 ps only, on the other hand. Thus a minor influence of the obstacles to the purely one-dimensional motion is observed in $\sigma_{\parallel}(T)$. As we mentioned in the introduction, a clean separation of $\sigma_{\parallel}(T)$ and $\sigma_{\perp}(T)$ is prevented by instrumental factors in microwave conductivity measurements. Nevertheless, even for the reduced 100:1 anisotropy figure 4 visualizes the more pronounced temperature dependent decay of $\sigma_{\perp}(T)$ in the temperature range below 170 K.

Pure transverse motion is difficult to ascertain for instrumental reasons. Here we pushed the experimental limit of the anisotropy of the diffusion coefficient, $D_{\parallel}{:}D_{\perp}$, to 7300:1. The temperature dependence of $D_{\parallel}(T)$ and $D_{\perp}(T)$ is different for $(PE)_2AsF_6{\cdot}\frac{2}{3}$ THF under these experimental conditions, but both show pronounced anomalies around $T_S \approx 170$ K, at variance with the microwave conductivity results for $\sigma_{\parallel}(T)$ and $\sigma_{\perp}(T)$ shown in figure 2. For temperatures above T_s, $D_{\perp}$ decreases with increasing temperatures, but allowing for the full error limit $D_{\perp}$ might also be temperature independent in the metallic high temperature phase. The crystal length of sample B of 320 μm is still large enough to render the influence of the unwanted perpendicular components of the magnetic field gradients possible [10]. A sequence of measurements for varied thickness of crystal slices is required for extrapolation of $D_{\perp}$ to vanishing instrumental distortion. This opens the possibility of a clear-cut separation of parallel- and perpendicular-to-stack motion for arene salts allowing a more systematic variation of the defect content (x_d) [19]. These comprehensive studies can only be realized for fluoranthene radical cation salts, not susceptible to uncontrolled sample variations caused by solvent inclusion in the crystal structure. Figure 5 shows that $D_{\perp}(T)$ decreases below the Peierls transition at $T_P \approx 103$ K and scatters around T_S, the structural phase transition of $(PE)_2AsF_6{\cdot}\frac{2}{3}$ THF. For $D_{\parallel}(T)$, this temperature dependence is enhanced by the accompanying decrease of $\overline{l}_{\parallel}(T)$.

4. Conclusions

The most relevant result of the present study is the rather pronounced decrease of the diffusion coefficient $D_{\parallel}(T)$ in the temperature range $T_S \geqslant T > T_P$, i.e. above the Peierls transition. This could be explained by the reduction of the finite chain length, $l_{\parallel}$, reflected by its average value $\overline{l}_{\parallel}(T)$ in the conduction electron spin-echo attenuation analysis (figure 4). This reduction of $\overline{l}_{\parallel}$ is explained by domain formation at the structural phase transition T_S, where neighbouring PE stacks rotate around their stacking axis in opposite directions. The shortened undisturbed chain segments, $l_{\parallel}$, enforce an increased number of transverse hoppings ($D_{\perp}$) in order to continue the motion along the preferred direction. Motion perpendicular to the stack, $D_{\perp}$, is shown to be strongly suppressed in quasi-one-dimensional conductors belonging to the arene radical cation salts, like $(PE)_2AsF_6{\cdot}\frac{2}{3}$ THF. The respective instrumental limit is pushed here to $D_{\parallel}{:}D_{\perp} \approx 7300{:}1$.

Acknowledgments

We thank I Odenwald for crystal growth and S Matejcek for experimental advice. This work was financially supported by the Deutsche Forschungsgemeinschaft (project DO 181/10).

References

[1] Pongs B, Fischer G and Dormann E 2002 *J. Phys.: Condens. Matter* **14** 8655
[2] Kaiser A, Wokrina T, Pongs B and Dormann E 2003 *J. Phys.: Condens. Matter* **15** 7085
[3] Feintuch A, Grayevsky A, Buschhaus C, Dormann E and Kaplan N 2004 *Curr. Appl. Phys.* **4** 373
[4] Burggraf M, Dragan H, Gruner-Bauer P, Helberg H W, Kuhs W F, Mattern G, Müller D, Wendl W, Wolter A and Dormann E 1995 *Z. Phys.* **96** 439
[5] Schaumburg G and Helberg H W 1994 *J. Physique* III **4** 917
[6] Wolter A, Fasol U, Jäppelt R and Dormann E 1996 *Phys. Rev.* B **54** 12272
[7] Feintuch A, Grayevsky A, Kaplan N and Dormann E 2004 *Phys. Rev. Lett.* **92** 156803
[8] Abragam A 1961 *The Principles of Nuclear Magnetism* (Oxford: Oxford University Press)
[9] Maresch G G, Grupp A, Mehring M, von Schütz J U and Wolf H C 1985 *J. Physique* **46** 461
[10] Wokrina T, Gmeiner J, Kaplan N and Dormann E 2003 *Eur. Phys. J.* B **35** 191
[11] Wokrina T, Dormann E and Kaplan N 1996 *Phys. Rev.* B **54** 10492
[12] Buschhaus C, Moret R, Ravy S and Dormann E 2000 *Synth. Met.* **108** 21
[13] Desquiotz R, Hofmann M and Dormann E 2000 *Eur. Phys. J.* B **16** 403
[14] Fischer G and Dormann E 1998 *Phys. Rev.* B **58** 7792
[15] Fischer G and Dormann E 2000 *Eur. Phys. J.* B **15** 21
[16] Tashma T, Alexandrowicz G, Kaplan N, Dormann E, Grayevsky A and Gabay A 1999 *Synth. Met.* **106** 151
[17] Warth A 2004 *Diplomarbeit* Universität Karlsruhe, unpublished
[18] Buschhaus C, Gmeiner J, Henke H, Ulrich M and Dormann E 2005 *Synth. Met.* **149** 89
[19] Drescher M, Saez de Jauregui D, Matejcek S and Dormann E 2005 *Synth. Met.* at press